Received: 20 June 2022 | Revised: 7 October 2022 | Accepted: 14 October 2022

DOI: 10.1002/eqe.3769

RESEARCH ARTICLE

WILEY

Conditional hazard for simplified multi-site seismic hazard and risk analyses

Pasquale Cito[1] | **Eugenio Chioccarelli**[2] | **Iunio Iervolino**[1]

[1]Dipartimento di Strutture per l'Ingegneria e l'Architettura, Università degli Studi di Napoli Federico II, Naples, Italy

[2]Dipartimento di Ingegneria Civile, dell'Energia, dell'Ambiente e dei Materiali, Università degli Studi Mediterranea di Reggio Calabria, Reggio Calabria, Italy

Correspondence
Iunio Iervolino, Dipartimento di Strutture per l'Ingegneria e l'Architettura, Università degli Studi di Napoli Federico II, Naples, Italy.
Email: iunio.iervolino@unina.it

Abstract

The joint probability distribution of different intensity measures (*IMs*) at different sites in one earthquake is needed to define the stochastic process regulating the exceedance (in time) of the *IMs* at the ensemble of the sites, which in turn is a funding element of the so-called multi-site probabilistic seismic hazard analysis (MSPSHA). The simplest model for the joint distribution of the *IMs* in one seismic event requires the mean vector and the covariance matrix of the *IMs* at all sites, conditional to the magnitude and location of the earthquake, which may need a large amount of data to be calibrated. The conditional hazard (CH) approach, originally developed for single-site surrogate vector-valued probabilistic seismic hazard analysis, may be a simplified option for MSPSHA, as it explicitly models only part of the covariance matrix of the *IMs* at the sites, while the rest forcefully follows the working assumptions. The presented paper compares the CH approach for MSPSHA against the benchmark in which the complete covariance matrix is modelled, using a testbed in which one-hundred sites are considered. When the comparison metric is the probability of a given number of *IM* exceedances observed at the sites in some time intervals, it is found that CH is a viable alternative to MSPSHA, although the degree of approximation is sensitive to which and how many *IMs* are considered (e.g., which spectral acceleration). When the analysis is taken all the way to the risk, considering the fragilities of a portfolio of hypothetical buildings, and taking as the metric the probability of observing a given number of structural failures in a time interval, it is found that the approximation introduced by CH with respect to the benchmark is further reduced.

KEYWORDS
distributed infrastructure, ground motion models, performance-based earthquake engineering, seismic fragility

1 | INTRODUCTION

Probabilistic seismic hazard analysis (PSHA)[1,2] enables obtaining the rate (i.e., mean number per time unit) of earthquakes causing exceedance of an intensity measure (*IM*) threshold at a site of interest. In fact, under the classical assumptions

of PSHA, such a rate completely defines the homogenous Poisson process (HPP) as the stochastic process of earthquakes causing exceedance of the threshold at the site. PSHA needs two main inputs: (i) the definition of the seismic source(s) affecting the site, including the probabilistic characterization of the earthquakes possibly occurring, in terms of magnitude and location, and (ii) the characterization of the conditional probability density function (PDF) of the considered IM at the site in one earthquake with given magnitude and location, that is typically addressed via ground motion prediction equations (GMPEs).

When the seismic risk assessment for a spatially distributed infrastructure (e.g., a buildings portfolio or a utility distribution network) is of concern,[3,4] it is typically required to model the stochastic process regulating the exceedances of IM thresholds at the multiple sites where the infrastructure is located; this is because the quantification of the seismic risk at the regional scale is primarily based on counting the number of exceedances of ground motion IMs at the considered sites (e.g., Esposito et al.[5]), regardless of the loss metric of interest. Such a process is not, in the general case, an HPP, even if so is the process at any of the sites, taken individually. This case is typically referred to as multi-site PSHA or MSPSHA,[6,7] which requires to model the joint PDF of the IMs at all the sites in one earthquake of given magnitude and location. In turn, this needs to define the covariance matrix of the IMs at the different sites, conditional to the earthquake features.[8,9] The covariance matrix entails modelling the stochastic dependence of residuals from GMPEs (to follow), via correlation models for: (i) different IMs at the same site (*cross*-correlation), (ii) the same IM at different sites (*spatial* correlation), (iii) different IMs at different sites (*spatial cross*-correlation). Several semi-empirical models for cross-correlation and spatial correlation can be found in literature,[3,10–14] but only a few for spatial cross-correlation are currently available.[15,16] In fact, the latter typically requires a relevant amount of region-dependent data to be calibrated via ground motion records.

The presented study investigates whether the modelling of the whole covariance matrix can be effectively approximated by a simpler approach based on the *conditional hazard*[17] (CH hereafter), which was originally developed in the framework of single-site PSHA and is virtually equivalent to *vector-valued* seismic hazard analysis.[18] CH allows to obtain the distribution of a *secondary IM* given a value of a *primary* one at the same site, provided that a cross-correlation model between the two IMs is at hand. CH can be extended to the multi-site case, if coupled with a spatial correlation model for the primary IM, to get the joint PDF of the IMs at the sites in one earthquake of given magnitude and location. The main advantage of this approach is that it does not require to define the whole covariance matrix of the IMs, at the cost of forcing its terms that are not directly assigned. In other words, it avoids the explicit modelling of: (i) the spatial cross-correlation among different IMs at different sites, (ii) the spatial correlation for the same secondary IM at different sites, and (iii) the cross-correlation among different secondary IMs at the same site (if more than one secondary IM is of interest). However, these correlations inherently follow from the CH hypotheses and can be seen as an approximation of the correlations they replace.

The effect of the strategy adopted to model the covariance matrix of the IMs on multi-site hazard and risk analyses has been investigated in literature;[8,9,19] however, a formalization of the implications of the considered approaches remains unaddressed and limits the generality of the conclusions. To provide a more general understanding of the CH-based MSPSHA, enabling to clarify its capabilities and limitations, is the aim of the presented study. This is carried out considering, as the *IMs*, some spectral accelerations corresponding to different vibration periods and, as testbed, one-hundred sites, which are assumed to represent the locations of hypothetical buildings within a portfolio covering an area about 200 km^2 wide in the district of Naples (southern Italy). The approximation implied by the CH is quantified first characterizing the stochastic process counting the number of exceedances of some sets of pre-defined IM thresholds collectively observed at the sites in different time intervals. The benchmark is the same analysis carried out implementing the whole covariance matrix of the IMs. The effect of CH on multi-site seismic risk analysis is also discussed considering the failure of hypothetical buildings located at the sites and modelled via seismic fragility functions.

The remainder of the paper is structured such that, after recalling the basics of MSPSHA and its main features, the state-of-the art to assign the covariance matrix of the different IMs at different sites in one earthquake is described. Subsequently, it is shown how some of the correlations needed for defining the covariance matrix can be approximated by the CH approach, if it is used together with a spatial correlation model for one of the IMs. It is also addressed how the CH inherently forces the correlations it does not require to assign. Consequently, the case-study comparisons in terms of multi-site hazard and risk analyses are shown and discussed. Some conclusions that can be drawn from the results close the study.

2 | MULTI-SITE PSHA

Let us start considering a number, s, of sites (i.e., s latitude-longitude pairs) and a number, z, of pseudo-spectral accelerations (Sa), that is, corresponding to z different vibration periods (i.e., z spectral accelerations per site). In the following, the symbol Sa_i^j will identify the acceleration at the generic site $j = 1, \ldots, s$ and corresponding to the vibration period

$i = 1, \dots, z$. A possible goal of MSPSHA is to count the number of exceedances of spectral acceleration thresholds collectively observed at all sites in a $(t, t + \Delta t)$ time interval, and the random variable (RV) of the stochastic process associated to this experiment can be indicated as $N(t, t + \Delta t)$.[20] It has been shown that, even if the exceedances of the thresholds in time at each site, taken individually, follow a HPP, the stochastic process counting exceedances at all the sites jointly does not generally follow a HPP, because the site-specific HPPs are not stochastically independent.[21] However, the mean and the variance of $N(t, t + \Delta t)$, that is, $E[N(t, t + \Delta t)]$ and $VAR[N(t, t + \Delta t)]$, respectively, can be computed as:

$$\begin{cases} E\left[N\left(t, t+\Delta t\right)\right] = \nu \cdot \Delta t \cdot \sum_{n=0}^{z \cdot s} n \cdot P\left[N = n\right] \\ VAR\left[N\left(t, t+\Delta t\right)\right] = \nu \cdot \Delta t \cdot \sum_{n=0}^{z \cdot s} n^2 \cdot P\left[N = n\right] \end{cases}, n = 0, 1, \dots, z \cdot s, \tag{1}$$

where ν denotes the annual rate of earthquakes on the sources affecting the sites (one seismic source is considered for the sake of simplicity) and $P[N = n]$ is the probability that the number of exceedances in a *generic* earthquake, that is, an earthquake with unspecified magnitude and location, is equal to $n = 0, 1, \dots, z \cdot s$. The latter probability can be computed via the *total probability theorem*:

$$P\left[N = n\right] = \int_M \int_X \int_Y P\left[N = n \,|m, x, y\,\right] \cdot f_{M,X,Y}\left(m, x, y\right) \cdot dm \cdot dx \cdot dy. \tag{2}$$

In the equation, $f_{M,X,Y}$ is the joint PDF of magnitude (M) and earthquake location $\{X, Y\}$ (e.g., the epicenter of the earthquake) given the occurrence of the earthquake; $P[N = n|m, x, y]$ is the conditional probability that, given an earthquake with magnitude and location equal to m and $\{x, y\}$, respectively, exactly n exceedances are jointly observed at the ensemble of the sites. Denoting as sa_i^{j*} the spectral acceleration threshold of interest for the $i-$th vibration period at the $j-$th site, $P[N = n|m, x, y]$ can be expressed as:

$$\begin{aligned} &P\left[N = n \,|m, x, y\,\right] = \\ &\int_{Sa_1^1} \dots \int_{Sa_z^s} I\left[\sum_{i=1}^{z} \sum_{j=1}^{s} I_{sa_i^j > sa_i^{j*}} = n\right] \cdot f_{Sa_1^1,\dots,Sa_z^s|M,X,Y}\left(sa_1^1, \dots, sa_z^s \,|m, x, y\,\right) \cdot d\left(sa_1^1\right) \cdot \dots \cdot d\left(sa_z^s\right), \end{aligned} \tag{3}$$

where $I_{sa_i^j > sa_i^{j*}}$ is an indicator function that equals one if sa_i^j is larger than sa_i^{j*} and zero otherwise, $I[\sum_{i=1}^{z} \sum_{j=1}^{s} I_{sa_i^j > sa_i^{j*}} = n]$ equals one if the sum of the indicator functions is equal to n and zero otherwise, and $f_{Sa_1^1,\dots,Sa_z^s|M,X,Y}$ is the joint PDF of all the spectral accelerations at all the sites conditional to the occurrence of an earthquake with given magnitude and location.

Because the spectral accelerations in one earthquake are not stochastically independent RVs, the modelling of $f_{Sa_1^1,\dots,Sa_z^s|M,X,Y}$ is a key element in MSPSHA. Therefore, there is a requirement to model the dependencies of all possible pairs of Sa_i^j and Sa_w^k, with $i = 1, \dots, z$, $j = 1, \dots, s$, $w = 1, \dots, z$ and $k = 1, \dots, s$. This issue is introduced in the following subsections via some basic examples of: (i) one site and one spectral acceleration, that is, $s = z = 1$; (ii) one site and multiple spectral accelerations; (iii) multiple sites and one spectral acceleration; (iv) multiple site and multiple spectral accelerations.

2.1 | One intensity measure at one site (PSHA essentials)

This section considers that one spectral acceleration (i.e., one vibration period), the $i-$th, at one site, the $j-$th, is of concern, that is, the case of single-site PSHA. The PDF of Sa_i^j, conditional to $\{m, x, y\}$, is typically derived via GMPE. Under the assumption that Sa_i^j is lognormally distributed, given magnitude and location of the earthquake, GMPEs model the logarithms of Sa_i^j as:

$$\log\left(Sa_i^j\right) = \mu_i^j\left(m, x, y, \underline{\theta}\right) + \sigma_i \cdot \varepsilon_i^j. \tag{4}$$

In the equation, $\mu_i^j(m,x,y,\underline{\theta})$ is the conditional mean of the logarithm of Sa_i^j given the occurrence of an earthquake with $\{m,x,y\}$, and additional covariates (e.g., site soil conditions, rupture mechanism, etc.) represented by the $\underline{\theta}$ vector. The elements of such a vector are usually not RVs, and therefore they are not considered in the following for the sake of simplicity. (Also note that, in the majority of the GMPEs, the conditional mean of $\log(Sa_i^j)$ depends, in fact, on a source-to-site distance metric rather than the earthquake location.) The $\sigma_i \cdot \varepsilon_i^j$ term is a zero mean and $(\sigma_i)^2$variance Gaussian RV; i.e., ε_i^j is the standardized residual that quantifies the number of standard deviations that the logarithm of Sa_i^j is far from the mean, given $\{m,x,y\}$ (for the majority of the GMPEs, the variance does not depend on the considered site, thus σ_i is here used as the symbol). Thus, once $\mu_i^j(m,x,y)$ and σ_i are known, the $f_{Sa_i^j|M,X,Y}$ PDF is completely defined and Equation (3) applies.

It has to be recalled herein that GMPEs usually present the residual divided into two terms, such that $\sigma_i \cdot \varepsilon_i^j = \phi_i \cdot \varepsilon_{i,\text{inter}}^j + \gamma_i \cdot \varepsilon_{i,\text{intra}}^j$. The $\phi_i \cdot \varepsilon_{i,\text{inter}}^j$ term is the inter-event residual, a Gaussian RV with zero mean and ϕ_i standard deviation. The term $\gamma_i \cdot \varepsilon_{i,\text{intra}}^j$ denotes the intra-event residual, a Gaussian RV with zero mean and γ_i standard deviation. Typically, inter- and intra-event residuals are assumed to be stochastically independent RVs, that is, the standard deviation of total residual is $\sigma_i = \sqrt{(\phi_i)^2 + (\gamma_i)^2}$. (Note that recent GMPEs, referred to as non-ergodic, and not explicitly considered herein, may present a different representation of the residual.)[22,23,24]

Before moving to the other cases, it is worthwhile observing that, when one spectral acceleration at one site is considered, the number of exceedances in one earthquake can only be equal to zero or one (i.e., a Bernoulli RV). Consequently, according to Equation (1), it is:

$$E\left[N\left(t,t+\Delta t\right)\right] = VAR\left[N\left(t,t+\Delta t\right)\right] = \nu \cdot \Delta t \cdot P\left[N=1\right], \tag{5}$$

where $P[N=1]$ is derived via Equation (2). Equation (5) shows that the mean and the variance of $N(t,t+\Delta t)$ are the same in this case. This means that the process counting the exceedances of sa_i^{j*} at the site in $(t,t+\Delta t)$ is an HPP characterized by an exceedance rate ($\lambda_{sa_i^{j*}}$) provided by Equation (6). In fact, this rate is the result of classical PSHA, and can be computed as:

$$\lambda_{sa_i^{j*}} = \nu \cdot P\left[N=1\right] = \nu \cdot P\left[Sa_i^j > sa_i^{j*}\right], \tag{6}$$

where $P[Sa_i^j > sa_i^{j*}]$ is the probability of exceeding the threshold at the site given the occurrence of a generic earthquake. Equation (6) is the so-called *hazard integral* (e.g., Kramer).[25]

2.2 | More than one intensity measure at one site

It is now considered the case in which z spectral ordinates are of interest at the (same) site; i.e., the $j-$th one. The sought PDF is therefore $f_{Sa_1^j,\ldots,Sa_z^j|M,X,Y}$. To compute it, it is typically assumed that the logarithms of the spectral ordinates at the site, given magnitude and location of the earthquake, are jointly Gaussian, that is, they follow a multivariate normal distribution. Thus, $f_{Sa_1^j,\ldots,Sa_z^j|M,X,Y}$ is defined via a conditional mean vector, $\underline{\mu}$, and a covariance matrix, $\underline{\underline{\Sigma}}$, as provided by Equation (7):

$$\begin{cases} \underline{\mu} = \left[\mu_1^j(m,x,y),\ldots,\mu_z^j(m,x,y)\right]^T \\ \underline{\underline{\Sigma}} = \underline{\underline{\Phi}} + \underline{\underline{\Upsilon}} = \begin{bmatrix} (\phi_1)^2 & \tau_{1,2}^{j,j}\cdot\phi_1\cdot\phi_2 & \cdots & \tau_{1,z}^{j,j}\cdot\phi_1\cdot\phi_z \\ & (\phi_2)^2 & \cdots & \vdots \\ & sym & \ddots & \vdots \\ & & & (\phi_z)^2 \end{bmatrix} + \begin{bmatrix} (\gamma_1)^2 & \varsigma_{1,2}^{j,j}\cdot\gamma_1\cdot\gamma_2 & \cdots & \varsigma_{1,z}^{j,j}\cdot\gamma_1\cdot\gamma_z \\ & (\gamma_2)^2 & \cdots & \vdots \\ & sym & \ddots & \vdots \\ & & & (\gamma_z)^2 \end{bmatrix}. \end{cases} \tag{7}$$

In the equation, $\underline{\mu}$ has z elements, one per spectral ordinate, each of which provided by the GMPE. The covariance matrix is given by the sum of two matrices, $\underline{\underline{\Phi}}$ and $\underline{\underline{\Upsilon}}$, each with $z \times z$ size, the terms of which include the correlations among inter- and intra-event residuals of the GMPE for the spectral accelerations at site j, respectively. More specifically, $\tau_{i,w}^{j,j}$

and $\varsigma_{i,w}^{j,j}$ denote the cross-correlation coefficient for inter- and intra-event residuals, respectively, considering all possible combinations of Sa_i^j and Sa_w^j, for $i = 1, \dots, z$ and $w = 1, \dots, z$ (if $i = w$, it is $\tau_{i,w}^{j,j} = \varsigma_{i,w}^{j,j} = 1$). According to literature, the cross-correlation of inter- and intra-event residuals decreases with the increasing difference of spectral periods the two spectral accelerations refer to,[11,14] sometimes in a magnitude-dependent manner.[26]

2.3 | One intensity measure at multiple sites

This section introduces the MSPSHA in which one spectral ordinate, that is, the $i-$th one, is of interest at all the s sites. In other words, $f_{Sa_i^1,\dots,Sa_i^s|M,X,Y}$ is sought. It is generally assumed that, given magnitude and location of the earthquake, the logarithms of the considered spectral acceleration at more than one site form a Gaussian random field or GRF.[27,28] Then, $f_{Sa_i^1,\dots,Sa_i^s|M,X,Y}$ is modelled via a conditional mean vector, $\underline{\mu}$, and a covariance matrix, $\underline{\underline{\Sigma}}$, as per Equation (8):

$$\begin{cases} \underline{\mu} = \left[\mu_i^1(m,x,y), \dots, \mu_i^s(m,x,y)\right]^T \\ \underline{\underline{\Sigma}} = \underline{\underline{\Phi}} + \underline{\underline{\Upsilon}} = \begin{bmatrix} (\phi_i)^2 & (\phi_i)^2 & \cdots & (\phi_i)^2 \\ & (\phi_i)^2 & \cdots & (\phi_i)^2 \\ & sym & \ddots & \vdots \\ & & & (\phi_i)^2 \end{bmatrix} + \begin{bmatrix} (\gamma_i)^2 & \varsigma_{i,i}^{1,2}\cdot(\gamma_i)^2 & \cdots & \varsigma_{i,i}^{1,s}\cdot(\gamma_i)^2 \\ & (\gamma_i)^2 & \cdots & \vdots \\ & sym & \ddots & \vdots \\ & & & (\gamma_i)^2 \end{bmatrix}. \end{cases} \tag{8}$$

In the considered case, the mean vector has s elements, one per site, each provided by the GMPE, while $\underline{\underline{\Phi}}$ and $\underline{\underline{\Upsilon}}$, each with $s \times s$ size, include the correlations among inter- and intra-event residuals of the GMPE for the $i-$th spectral acceleration at the sites, respectively. More specifically, the $\underline{\underline{\Phi}}$ matrix shows that the same inter-event residual is shared by all sites in one seismic event; i.e., they are perfectly correlated in one earthquake. The $\underline{\underline{\Upsilon}}$ matrix includes the spatial correlation of intra-event residuals at the different sites that, according to literature, decreases with the increasing inter-site distance.[3,12] In fact, $\varsigma_{i,i}^{j,k}$ denotes the spatial correlation coefficient between the intra-event residuals of the GMPE, considering the $i-$th spectral acceleration at sites j and k, for $j = 1, \dots, s$ and $k = 1, \dots, s$ (if $k = j$, $\varsigma_{i,i}^{j,k} = 1$).

It should be noted, at this point, that non-ergodic GMPEs provide the spatial correlation model of residuals, which is not included in classical GMPEs, for one intensity measure. However, they do not typically account for spatial cross-correlation (see next section).

2.4 | More than one intensity measure at multiple sites

In the most general case, the MSPSHA deals with z spectral ordinates at each of the s sites. In this situation, the hypothesis of joint lognormality, conditional to the earthquake magnitude and location, is usually taken referring to all the spectral ordinates at all the sites. Therefore $f_{Sa_1^1,\dots,Sa_z^s|M,X,Y}$ is a conditional multivariate lognormal distribution, the mean vector and covariance matrix of which are defined as per Equation (9):

$$\begin{cases} \underline{\mu} = \left[\mu_1^1(m,x,y), \dots, \mu_z^s(m,x,y)\right]^T \\ \underline{\underline{\Sigma}} = \underline{\underline{\Phi}} + \underline{\underline{\Upsilon}} = \\ \begin{bmatrix} (\phi_1)^2 & \cdots & \tau_{1,1}^{1,s}\cdot(\phi_1)^2 & \cdots & \tau_{1,z}^{1,1}\cdot\phi_1\cdot\phi_z & \cdots & \tau_{1,z}^{1,s}\cdot\phi_1\cdot\phi_z \\ \ddots & & \vdots & \cdots & & \cdots & \vdots \\ & & (\phi_1)^2 & \cdots & \tau_{1,z}^{s,1}\cdot\phi_1\cdot\phi_z & \cdots & \tau_{1,z}^{s,s}\cdot\phi_1\cdot\phi_z \\ & & & & & \cdots & \vdots \\ & & & \ddots & (\phi_z)^2 & \cdots & \tau_{z,z}^{1,s}\cdot\phi_z\cdot\phi_z \\ & & & & & \ddots & \vdots \\ & sym & & & & & (\phi_z)^2 \end{bmatrix} + \begin{bmatrix} (\gamma_1)^2 & \cdots & \varsigma_{1,1}^{1,s}\cdot(\gamma_1)^2 & \cdots & \varsigma_{1,z}^{1.1}\cdot\gamma_1\cdot\gamma_z & \cdots & \varsigma_{1,z}^{1,s}\cdot\gamma_1\cdot\gamma_z \\ \ddots & & \vdots & \cdots & & \cdots & \vdots \\ & & (\gamma_1)^2 & \cdots & \varsigma_{1,z}^{s,1}\cdot\gamma_1\cdot\gamma_z & \cdots & \varsigma_{1,z}^{s,s}\cdot\gamma_1\cdot\gamma_z \\ & & & \cdots & \vdots & \vdots & \vdots \\ & & & \ddots & (\gamma_z)^2 & \cdots & \varsigma_{z,z}^{1,s}\cdot(\gamma_z)^2 \\ & & & & & \ddots & \vdots \\ & sym & & & & & (\gamma_z)^2 \end{bmatrix}. \end{cases} \tag{9}$$

In this case, $\underline{\mu}$, has $z \cdot s$ elements, one for each site and spectral acceleration according to the GMPE. The covariance matrix, $\underline{\underline{\Sigma}}$, is somewhat more elaborated than the previous cases, as the $\underline{\underline{\Phi}}$ and $\underline{\underline{Y}}$ matrices have $z \cdot s \times z \cdot s$ size. In fact, $\underline{\underline{\Sigma}}$ considers all possible combinations of Sa_i^j and Sa_w^k, that is, with $i = 1, \dots, z$, $j = 1, \dots, s$, $w = 1, \dots, z$ and $k = 1, \dots, s$. More specifically, $\tau_{i,w}^{j,k}$ denotes the spatial cross-correlation coefficient between the inter-event residuals of the GMPE, considering Sa_i^j and Sa_w^k. Such a coefficient does not depend on the inter-site distance, that is, $\tau_{i,w}^{j,k}$ is the same for each (j,k) pair, and it is also $\tau_{i,w}^{j,k} = 1$ if $i = w$. The $\varsigma_{i,w}^{j,k}$ term is the spatial cross-correlation coefficient between intra-event residuals of the GMPE for Sa_i^j and Sa_w^k. If $i = w$, $\varsigma_{i,i}^{j,k}$ ($\varsigma_{w,w}^{j,k}$) is the spatial correlation coefficient for intra-event residuals considering the $i-$th ($w-$th) spectral acceleration at sites j and k. If $k = j$, $\varsigma_{i,w}^{k,k}$ ($\varsigma_{i,w}^{j,j}$) represents the cross-correlation coefficient between intra-event residuals of the GMPE for the $i-$th and $w-$th spectral acceleration at site k (j). Finally, if $k = j$ and $i = w$, it is $\varsigma_{i,w}^{j,k} = 1$. According to literature, the spatial cross-correlation of intra-event residuals tends to decrease with the increasing inter-site distance and the increasing difference between the spectral periods.[15,16] It is easy to acknowledge that Equation (9) is a generalization of all the previously discussed cases.

Once the mean vector and the covariance matrix of the distribution of the spectral accelerations at all sites, conditional to the earthquake features, are described, $f_{Sa_1^1,\dots,Sa_2^s|M,X,Y}$ is known and MSPSHA can be performed (see Section 2). Because the covariance matrix is completely defined, the implementation according to the shown equations is denoted as *explicit* approach, to distinguish it by the one discussed in the next section, as it will be readily understood.

3 | CONDITIONAL HAZARD

It has been recalled that, given magnitude and location of the earthquake, the logarithm of the spectral accelerations at the sites are assumed to be jointly Gaussian. When two spectral accelerations at one site, say j, are of concern, the covariance matrix is given by Equation (7) (for $z = 2$), which is factually part of the one provided by Equation (9) for multiple sites ($s > 1$) and spectral accelerations ($z > 1$). In such a case, conditional to a value of Sa_1^j, which is arbitrarily indicated as the *primary* intensity measure, and the earthquake's magnitude and location, it is easy to derive the conditional distribution of Sa_2^j, indicated as the *secondary* intensity measure.[17] The logarithm of Sa_2^j given the occurrence of a value of Sa_1^j, indicated as sa_1^j, and the earthquake's magnitude and location, is distributed according to a Gaussian distribution with parameters provided by:

$$\begin{cases} \mu_2^j\left(m,x,y,sa_1^j\right) = \mu_2^j(m,x,y) + \sigma_2 \cdot \rho_{1,2}^{j,j} \cdot \frac{\log\left(sa_1^j\right) - \mu_1^j(m,x,y)}{\sigma_1} \\ \sigma_2\left(sa_1^j\right) = \sigma_2 \cdot \sqrt{1 - \left(\rho_{1,2}^{j,j}\right)^2} \end{cases}. \tag{10}$$

In the equation, $\mu_2^j(m,x,y,sa_1^j)$ and $\sigma_2(sa_1^j)$ are the conditional mean and standard deviation of the logarithm of Sa_2^j, respectively. The $\rho_{1,2}^{j,j}$ is the cross-correlation coefficient between the total residuals of the GMPE of the two spectral accelerations at the same site. It can be expressed as:

$$\rho_{1,2}^{j,j} = \frac{\tau_{1,2}^{j,j} \cdot \phi_1 \cdot \phi_2 + \varsigma_{1,2}^{j,j} \cdot \gamma_1 \cdot \gamma_2}{\sqrt{(\phi_1 \cdot \phi_2)^2 + (\phi_1 \cdot \gamma_2)^2 + (\gamma_1 \cdot \phi_2)^2 + (\gamma_1 \cdot \gamma_2)^2}}, \tag{11}$$

where all the terms have been already defined. In fact, the numerator is the covariance between total residuals of the GMPE referring to Sa_1^j and Sa_2^j, while the denominator is factually the product of σ_1 and σ_2; see also Equation (7).

3.1 | Conditional hazard based MSPSHA

This section shows that the CH approach can be also used in the context of MSPSHA, when multiple spectral accelerations are considered. Similar to the previous section, the primary Sa at site $j = 1, \dots, s$ is denoted as Sa_1^j. Then, each of the other

spectral accelerations at the sites is intended as a secondary intensity measure, and it is indicated in the following as Sa_i^j, with $i = 2, \dots, z$.

Conditional-hazard-based MSPSHA assumes that the primary spectral acceleration is the same at all the sites (i.e., the spectral acceleration for the same vibration period). Once it is selected, the correlations explicitly considered are only two: (i) a spatial correlation model for the primary spectral acceleration at the sites, that is, Sa_1^j, $j = 1, \dots, s$, and (ii) the cross-correlation model between Sa_1^j and Sa_i^j, with $i = 2, \dots, z$ and $j = 1, \dots, s$. In other words, the spatial cross-correlation between the primary and the secondary spectral accelerations at different sites, the spatial correlation, as well as the cross-correlations, of secondary spectral accelerations are not assigned. Then, the CH-based MSPSHA can be summarized in the following procedure.

(1) The joint lognormal distribution of the primary spectral acceleration at the different sites conditional on magnitude and location of the earthquake, $f_{Sa_1^1,\dots,Sa_1^s|M,X,Y}$, is computed accounting for the spatial correlation via Equation (8).
(2) At the $j-$th site, $j = 1, \dots, s$, all the secondary spectral accelerations are assumed to be stochastically independent conditionally to earthquake's magnitude and location, and the primary spectral acceleration at the same site. Therefore, the conditional joint distribution of the ensemble of the secondary spectral ordinates can be obtained as:

$$f_{Sa_2^j,\dots,Sa_z^j|Sa_1^j,M,X,Y}\left(sa_2^j, \dots, sa_z^j \,\middle|\, sa_1^j, m, x, y\right) = \prod_{i=2}^{z} f_{Sa_i^j|Sa_1^j,M,X,Y}\left(sa_i^j \,\middle|\, sa_1^j, m, x, y\right). \tag{12}$$

In the equation, $f_{Sa_i^j|Sa_1^j,M,X,Y}, i = 2, \dots, z$ represents a lognormal distribution, with parameters (of the logs) given in Equation (10).
(3) Given the earthquake features and the primary spectral ordinate at the $j-$th site, any of the secondary at that site, Sa_i^j, with $i = 2, \dots, z$ and $j = 1, \dots, s$, is considered stochastically independent of any other secondary spectral ordinate at any other site, Sa_w^k, for $w = 2, \dots, z$ and $k = 1, \dots, s$, with $(k \neq j)$. This allows to get the conditional distribution of all secondary spectral ordinates at all the sites as:

$$f_{Sa_2^1,\dots,Sa_z^s|Sa_1^1,\dots,Sa_1^s,M,X,Y}\left(sa_2^1, \dots, sa_z^s \,\middle|\, sa_1^1, \dots, sa_1^s, m, x, y\right) = \prod_{j=1}^{s} f_{Sa_2^j,\dots,Sa_z^j|Sa_1^j,M,X,Y}\left(sa_2^j, \dots, sa_z^j \,\middle|\, sa_1^j, m, x, y\right). \tag{13}$$

(4) The joint distribution of the z spectral ordinates at the s sites, conditional on earthquake magnitude and location, then is finally obtained as:

$$\begin{aligned} &f_{Sa_1^1,\dots,Sa_z^s|M,X,Y}\left(sa_1^1, \dots, sa_z^s \,|m, x, y\right) = \\ &= f_{Sa_2^1,\dots,Sa_z^s|Sa_1^1,\dots,Sa_1^s,M,X,Y}\left(sa_2^1, \dots, sa_z^s \,\middle|\, sa_1^1, \dots, sa_1^s, m, x, y\right) \cdot f_{Sa_1^1,\dots,Sa_1^s|M,X,Y}\left(sa_1^1, \dots, sa_1^s \,|m, x, y\right) \end{aligned}. \tag{14}$$

3.2 | Implicit correlations

It has been shown that the CH procedure allows to derive the joint distribution of the spectral ordinates at the sites in one earthquake with given magnitude and location without explicitly assigning some of the correlations of the GMPE residuals listed in Section 2.4, that is, spatial cross-correlations, spatial correlation and cross-correlation for the secondary spectral ordinates. Therefore, when MSPSHA is of concern, implementing CH, in lieu of the explicit approach, reduces the number of terms to be defined for modelling the covariance matrix of the spectral accelerations at the sites. On one hand, this can be considered a main advantage; on the other hand, the CH approach implicitly assigns, in an approximated manner, the neglected correlations. It can be demonstrated that the following correlations of total residuals result as a

combination of those modelled at steps 1 and 2 illustrated in the previous section:

$$\begin{cases} \rho_{1,i}^{j,k} = \rho_{1,i}^{j,j} \cdot \rho_{1,1}^{j,k} \\ \rho_{i,i}^{j,k} = \left(\rho_{1,i}^{j,j}\right)^2 \cdot \rho_{1,1}^{j,k} \\ \rho_{i,w}^{j,k} = \rho_{1,i}^{j,j} \cdot \rho_{1,w}^{j,j} \cdot \rho_{1,1}^{j,k} \\ \rho_{i,w}^{j,j} = \rho_{1,i}^{j,j} \cdot \rho_{1,w}^{j,j} \cdot \left(\rho_{1,1}^{j,k}\right)^2 \end{cases}, i = 2, \dots, z; w = 2, \dots, z\,(i \neq w); k = 1, \dots, s; j = 1, \dots, s\,(k \neq j)\,. \tag{15}$$

It is remarked that the cross-correlation coefficient between two different spectral accelerations at the same site does not vary with the site it refers to; in other words, $\rho_{1,i}^{j,j}$ ($\rho_{1,w}^{j,j}$) is the same as $\rho_{1,i}^{k,k}$ ($\rho_{1,w}^{k,k}$).

It should be noted that the first of Equation (15) was already presented by Goda and Hong.[15] Considering the case of two different spectral ordinates at two sites (one per site), they suggested that, to reduce the difference between the value of $\rho_{1,i}^{j,k}$ computed via the implicit approach and the corresponding value provided by a specifically-evaluated model of spatial cross-correlation, the primary spectral ordinate should be the one associated to the largest vibration period among the two of interest. Based on that, Weatherill et al.[8] recommend to use the longer period spectral acceleration as the primary one in the CH, also when several (i.e., more than two) spectral ordinates at multiple sites are of interest.

4 | MSPSHA VIA SIMULATION

In this section it is discussed how $P[N = n|m, x, y]$, which is needed to derive the MSPSHA result considered in this study (see Section 5), can be obtained via simulations. Indeed, sampling the (logs of) acceleration values from $f_{Sa_1^1,\dots,Sa_z^s|M,X,Y}$ an arbitrary number of times, say R, $P[N = n|m, x, y]$ is approximated by the number of times in which the realizations of the multivariate Gaussian distribution gives n exceedances, as:

$$P\left[N = n\,|m, x, y\,\right] \approx \frac{\sum_{r=1}^{R}\left\{I\left[\sum_{i=1}^{z}\sum_{j=1}^{s} I_{sa_i^j > sa_i^{j*}} = n\right]\right\}_r}{R}, \tag{16}$$

where the indicator functions are the same introduced by Equation (3). The way in which the numerical simulations are performed can be consistent with the explicit or the CH approach. In words, the only difference between the two MSPSHA procedures is in the $f_{Sa_1^1,\dots,Sa_z^s|M,X,Y}$ joint distribution, from which the values of sa_i^j, with $i = 1, \dots, z$ and $j = 1, \dots, s$, are sampled. In the following, it is shown how to simulate the values of z spectral ordinates at s sites, given magnitude and earthquake location, according to the explicit or the CH procedure. (Note that, in principle, the simulated realizations of the spectral ordinates at the sites can be used to derive any MSPSHA results.)

4.1 | Explicit approach

As pertaining to the explicit approach, given the magnitude and the location of the earthquake, the following steps can be followed for the $r-$th simulation, $r = 1, \dots, R$:

(i) the vector of conditional averages at the sites in Equation (9) is computed according to the considered GMPEs;
(ii) the realizations of the residuals of the GMPEs at the sites for all intensity measures ($z \cdot s$ realizations) are sampled from a multivariate normal distribution with zero mean and covariance matrix as per Equation (9);
(iii) summing up the sampled residuals (step ii) to the corresponding mean values (step i), gives the realizations of the logarithms of the z spectral accelerations at the s sites given $\{m, x, y\}$;
(iv) the values resulting from step iii form a realization of $f_{Sa_1^1,\dots,Sa_z^s|M,X,Y}$ that is used to check whether n exceedances are observed or not, given $\{m, x, y\}$.

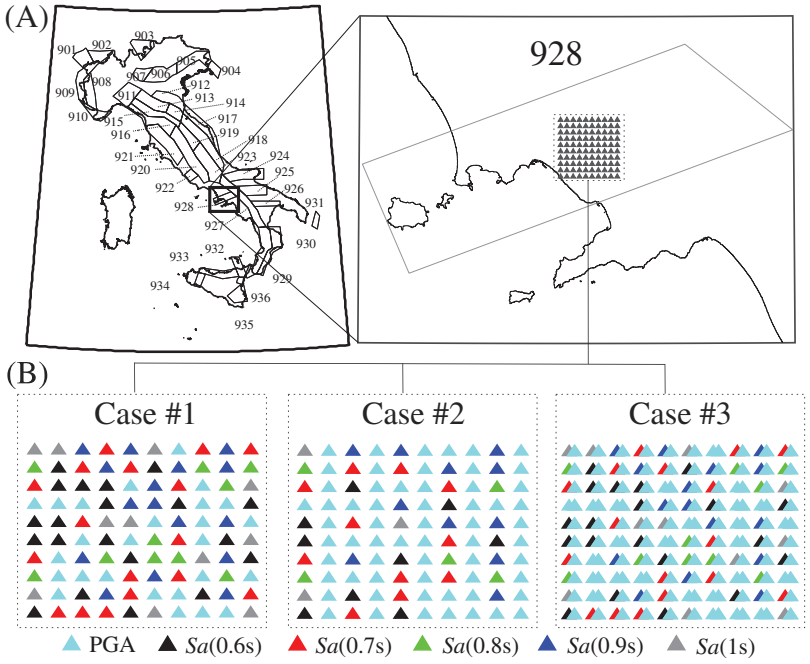

FIGURE 1 Seismic source and sites (tringles) considered in the analyses (A); intensity measures (triangle colors) considered in the different MSPSHA cases (B)

4.2 | Conditional hazard

In the case of the CH-based MSPSHA, the spectral acceleration to be considered as primary at each site has to be selected first. Then, given magnitude and earthquake location, the $r-$th simulation proceeds as follows:

(i) the vector of conditional averages, of the primary spectral acceleration, at the sites in Equation (8) is computed according to the considered GMPEs;
(ii) the realizations, s in number, of the residuals of the GMPEs for the primary spectral acceleration at the sites are sampled from a multivariate normal distribution with zero mean and covariance matrix as per Equation (8);
(iii) summing up the sampled residuals (step ii) to the means (step i) gives the realizations of the GRF for the logarithms of the primary spectral acceleration at the sites, given $\{m, x, y\}$;
(iv) at each $j-$th site, $j = 1, \dots, s$, the lognormal distribution of $Sa_i^j, i = 2, \dots, z$, conditional to $\{m, x, y\}$ and the realization of Sa_1^j, $f_{Sa_i^j|Sa_1^j,M,X,Y}$, is obtained by means of Equation (10);
(v) sampling from each $f_{Sa_i^j|Sa_1^j,M,X,Y}$, $i = 2, \dots, z$ and $j = 1, \dots, s$, provides the realizations of the logarithms of the z spectral accelerations at the s sites given $\{m, x, y\}$ and sa_1^j;
(vi) the realizations of the primary spectral accelerations from step iii and those obtained at step v provide the $r-$th realization of the $f_{Sa_1^1,\dots,Sa_z^s|M,X,Y}$ joint PDF, which is used to check whether n exceedances are observed or not, given $\{m, x, y\}$.

5 | EFFECTS OF CONTIONAL HAZARD APPROXIMATION ON MSPSHA

It has been discussed that the use of CH approximates the covariance matrix of the spectral accelerations at the sites in a given earthquake, with respect to the (explicit) case in which all correlations are assigned. The aim of this section is to provide a quantitative measure of the effect of such approximations on MSPSHA results. The number of exceedances over time of ground motion intensity measure thresholds for a set of sites is analyzed; that is, $N(t, t + \Delta t)$. The thresholds are in terms of spectral accelerations corresponding to different natural vibration periods. The sites, which are assumed to be representative of the locations of hypothetical buildings within a portfolio covering an about 200 km^2 wide area, are one hundred (i.e., $s = 100$). They are distributed on a regular grid with nodes spacing equal to 1.5 km and are located in the district of Naples (southern Italy); see Figure 1A. (The sensitivity of this kind of analysis to the inter-site distance was

investigated in a previous work,[19] showing that it is limited.) Different time intervals are considered in the analyses: 50, 100, and 150 years.

Because the measured approximations are substantially dependent on the MSPSHA setting, three cases of analysis (i.e., portfolio configurations) are considered to quantitatively discuss the sensitivity of approximations to the vibration period of the spectral ordinates of interest and to the number of spectral ordinates per site. Case #1 (to follow) is assumed as a benchmark case, case #2 and case #3 are built to amplify the approximations related to the CH approach with respect to case #1. More specifically, each case is characterized as follows.

- Case #1. For each site, one spectral acceleration (i.e., $z = 1$) is (arbitrarily) selected among Sa(0s), Sa(0.6s), Sa(0.7s), Sa(0.8s), Sa(0.9s) and Sa(1s), being Sa(0s) the peak ground acceleration (PGA). In Figure 1B, the spectral acceleration selected at each site is represented via color-coding; as shown, none of the considered spectral ordinates are predominant in number with respect to the others. Moreover, at all the sites, the spectral ordinate selected as the primary one, in accordance with the CH approach, is Sa(1s), that is, the one characterized by the largest vibration period among those considered. The choice of the primary intensity measure is in accordance with what suggested by literature[8,15] and factually motivates the characteristics of the other cases.
- Case #2. Similar to the previous case, one spectral acceleration per site is considered, and Sa(1s) is the primary intensity measure at each site for the CH approach. However, this case is intended to investigate how the approximations of CH vary increasing the number of sites in which the lowest vibration period spectral acceleration is considered, that is, PGA. As shown in Figure 1B, PGA is considered for 61% and 25% of sites in case #2 and case #1, respectively.
- Case #3. For each site, two spectral accelerations (i.e., $z = 2$) are considered. As shown in Figure 1B, one is the same as in case #1, while the other is PGA at each site. The primary intensity measure selected within CH remains Sa(1s). Thus, similar to case #2, case#3 is obtained via a modification of case #1 and is intended to increase the number of implicit correlations when CH is implemented.

The seismic source model used in the analyses was taken from the model for Italy of Meletti et al.[29] More specifically, the source zone (named 928 in the cited model) is considered (Figure 1A). In accordance with Barani et al,[30] the zone is characterized by a magnitude distribution of events following a Gutenberg-Richter (GR) model.[31] The minimum and maximum magnitude is equal to 4.3 and 5.8, respectively. The b parameter of the GR model is equal to 1.056. The rate of earthquakes above the minimum magnitude is $\nu = 0.054$ events per year. According to Meletti et al.,[29] the normal style of faulting is considered as dominant in the source. The adopted GMPE is that of Akkar and Bommer,[32] which applies in the 5.0-7.6 magnitude range and Joyner and Boore[33] distance, or R_{JB}, (i.e., the metric of the GMPE) up to 100 km. It is assumed a uniform distribution of earthquakes' epicenter within the source and the earthquake epicentral distance from each site is converted to R_{JB} according to Montaldo et al.[34] Moreover, magnitude lower than 5.0 are neglected in the analysis to avoid GMPE extrapolation; thus, ν is reduced to 0.0092 events per year, according to the GR, to exclude earthquakes with magnitude between 4.3 and 5.0. Rock soil condition is assumed for all the sites. Cross-, spatial- and spatial cross-correlations among residuals of the GMPE were implemented by using the model of Baker and Jayaram[11] and Loth and Baker[16] for inter-event and intra-event terms, respectively. These models, as well as the selected GMPE, are considered applicable in the active shallow crustal setting of Italy.

The mean and variance of $N(t, t + \Delta t)$ are obtained considering three time intervals, that is, 50, 100, and 150 years (the definition of the intensity thresholds at the sites is detailed in the following section). Analyses were developed using explicit and CH-based MSPSHA. The analyses were carried out via the REASSESS[35] software for the explicit approach and with ad-hoc script for the CH-based MSPSHA.

Because the mean number of exceedances jointly observed at the sites is not affected by the covariance matrix of the spectral accelerations, the effect of CH is quantified by measuring the difference between the variances of the exceedances obtained through the explicit approach, $VAR[N(t, t + \Delta t)]$, assumed as a benchmark, and the CH, $VAR[N(t, t + \Delta t)]_{CH}$, that is, $\Delta = VAR[N(t, t + \Delta t)] - VAR[N(t, t + \Delta t)]_{CH}$.

5.1 | Intensity measure thresholds

This section describes the strategy adopted to define the thresholds at the sites needed for counting exceedances. Since the selected thresholds influence the differences between CH and explicit approach (as also shown in the following), the aim of this section is to identify the thresholds to make results of the analyses as general as possible. Thus, classical PSHA was

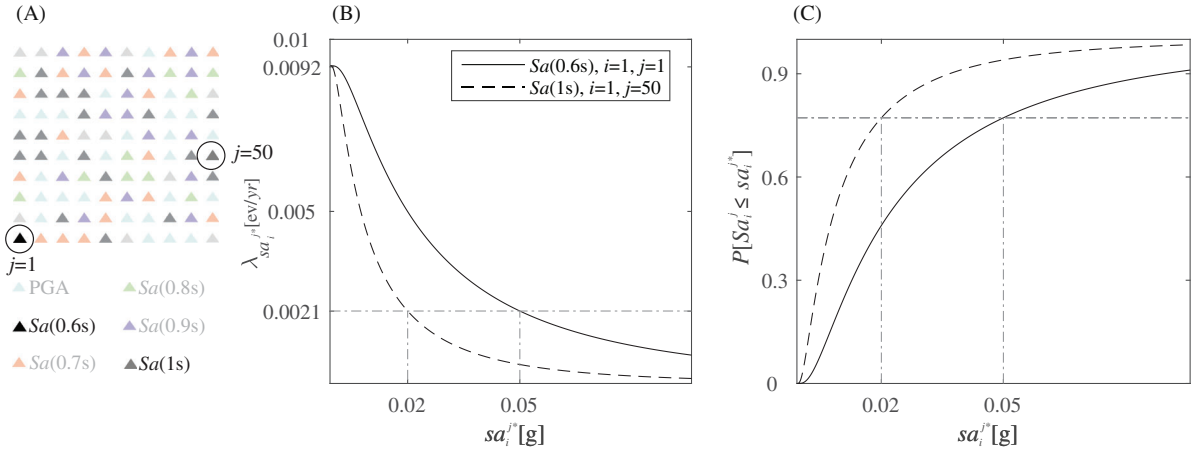

FIGURE 2 Sites and spectral accelerations according to case #1 (A); hazard curves for site 1 and 50 (B); curves of non-exceedance probability conditional to the occurrence of one generic earthquake (C)

performed for each site and spectral acceleration, first. In other words, for the $j-$th site and the $i-$th spectral acceleration, with $j = 1, \dots, 100$ and $i = 1, 2$, $\lambda_{sa_i^{j*}}$ was computed for different threshold values, obtaining the site-specific hazard curves, already introduced by Equation (6). To give an example, in Figure 2A, two sites are selected among the one-hundred introduced in the previous section; the corresponding annual hazard curves computed for the spectral accelerations considered in case #1 are shown in Figure 2B. More specifically, the curve for $j = 1$ and $i = 1$ is in terms of $Sa(0.6s)$, while the one for $j = 50$ and $i = 1$, is in terms of $Sa(1s)$.

One possible choice for threshold selection could be to identify the sa_i^{j*} value corresponding to a pre-defined exceedance rate, the same for all the sites, or equivalently to the same exceedance return period (T_r) (i.e., the reciprocal of the exceedance rate). This is represented in Figure 2B, in which the horizontal line associated to an (arbitrarily selected) exceedance rate equal to 0.0021 events per year, that is $T_r = 475yr$, identifies the values of the thresholds at the two considered sites. However, this choice would make results dependent on the rate characterizing the seismic source, ν; see also Equation (6). To avoid such a dependency, the thresholds are chosen to correspond to a certain probability of non-exceedance given the occurrence of a generic earthquake, $p = P[Sa_i^j \le sa_i^{j*}]$. In fact, p can be obtained from the hazard curve as $p = 1 - P[Sa_i^j > sa_i^{j*}] = 1 - \lambda_{sa_i^{j*}}/\nu$; see Equation (6). The curves of $P[Sa_i^j \le sa_i^{j*}]$, for the two considered sites and spectral ordinates, are reported in Figure 2C. The figure shows that, in this case, the accelerations corresponding to $p = 0.78$ are those with $T_r = 475yr$. Thus, in the following examples, the intensity thresholds are selected considering the same p at all sites.

5.2 | Effect of CH in different time intervals

This section quantifies the effect of the CH approach in computing the variance of the exceedances jointly observed at the one-hundred sites given the occurrence of multiple earthquakes in different time intervals, that is, 50, 100, and 150 years. Recalling that the variance of the exceedances in any time interval can be obtained via Equation (1), the sought Δ corresponds to:

$$\Delta = VAR\left[N\left(t, t+\Delta t\right)\right] - VAR[N\left(t, t+\Delta t\right)]_{CH} = \nu \cdot \Delta t \cdot \left\{ \sum_{n=0}^{z \cdot s} n^2 \cdot P\left[N = n\right] - \sum_{n=0}^{z \cdot s} n^2 \cdot P[N = n]_{CH} \right\}, \tag{17}$$

where $P[N = n]$ and $P[N = n]_{CH}$ represent the probability of observing n exceedances at the sites in one generic earthquake (see Section 2), according to the explicit and CH approach, respectively.

For each Δt, Δ is computed for different values of p identifying the thresholds at the sites (see the previous section). The curves of Δ as a function of p pertaining to case #1, case #2 and case #3 are reported in Figure 3A, Figure 3B, and Figure 3C, respectively. As shown, for any p, and for any case of analysis, Δ is always larger than zero. This means that the

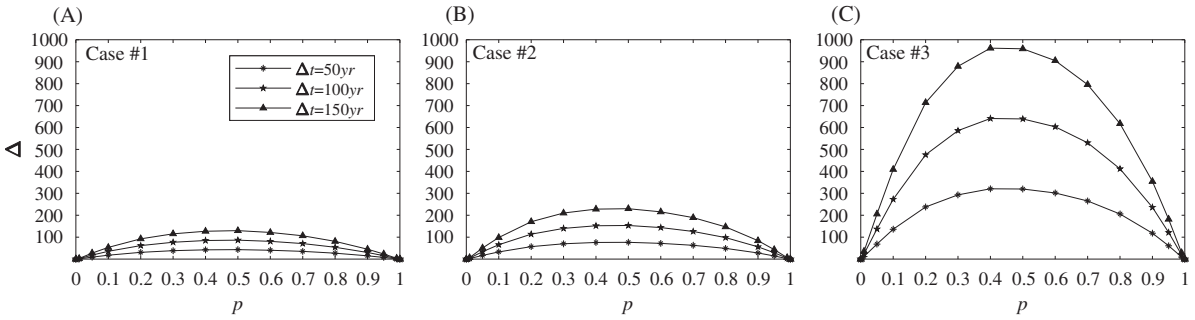

FIGURE 3 Effect of CH in MSPSHA in terms of Δ for case #1 (A), case #2 (B), and case #3 (C)

variation in the covariance matrix of the spectral accelerations at the sites due to the approximations introduced by CH causes an underestimation of the variance of the number of exceedances observed at the sites in the time interval. Also, as known from Equation (17), Δ linearly increases with Δt.

Figure 3 also shows that Δ varies with the increasing of p, that is, with the increasing of the thresholds at the sites. For any case of analysis and Δt, the curve starts from zero (when p tends to zero), increases for increasing values of p, reaches the maximum at the abscissa between 0.4 and 0.5 (depending on the case)* and decreases to zero when p approaches to one. This is because, considering very-low or -high thresholds, exceedances due to earthquakes, regardless of their magnitude and location, are observed at all sites and none of them, respectively, independently on the adopted MSPSHA procedure; therefore $VAR[N(t, t+\Delta t)]$ tends to be equal to $VAR[N(t, t+\Delta t)]_{CH}$ (and Δ tends to zero). (See also Section 5.3.)

Comparing the results for the three cases computed for the same Δt, it can be observed that Δ for case #2 is about twice that for case #1, for any p. For example, for the largest Δt, Δ increases from about 100 to about 200. This is because, as previously described, in case #2 the number of sites in which exceedances are counted referring to PGA is increased (61% of the whole set) with respect to case #1 (25% of the whole set). Thus, in case #2 the number of correlations that are implicitly modelled with CH is larger than case #1; that is, Equation (15). These are the spatial cross-correlation between PGA and Sa(1s), and spatial correlation among PGA at different sites. Finally, in case #3, Δ can be as high as (about) one thousand. In fact, given Δt, the ratio between the Δ value for case #3 and that for case #1 is between seven and eight, depending on p. This is because, in case #3, PGA is also of interest at each site and the correlations implicitly modelled with CH, already discussed for case #2, are further increased. Moreover, since two spectral ordinates are considered per site, results of case #3 are also influenced by the approximated correlations between two secondary spectral ordinates at the same site (see Section 3.2). Such results suggest that, in the CH approach to MSPSHA, choosing as primary intensity measure the spectral ordinate with the largest vibration period (which is, as also discussed in Section 3.2, the suggested choice) may produce significant approximations (in terms of Δ) when most of the spectral ordinates of interest correspond to low vibration periods (PGA in the case analyzed here).

5.3 | Effect of CH in one generic earthquake

This section is aimed at giving insights on the shape of the Δ curves in Figure 3. To do so, it has to be recalled that, according to Equation (17), the $\Delta/(\nu \cdot \Delta t)$ ratio gives the difference between the variance of the exceedance distributions in one generic earthquake computed via the explicit and the CH approaches; i.e., $P[N=n]$ and $P[N=n]_{CH}$, respectively. Denoting, for simplicity, such a ratio as Δ_E, it can be argued that the Δ curves represented in the previous section are exactly the Δ_E curves, scaled by different $\nu \cdot \Delta t$ factors (i.e., one per time interval). For this reason, considering the spectral ordinates of case #1, Figure 4A shows the trend of Δ_E as a function of p. The curve is slightly right-skewed and can be obtained by means of the law of the total variance,[36] according to which Δ_E is the weighted sum of the Δ_E values computed individually for each earthquake's magnitude and location involved in the computation of $P[N=n]$ (see Section 2). This is represented in Figure 4B, where the curve in panel A divided by its maximum, $\Delta_{E,\max}$, is shown: for each abscissa, the

* In fact, the finer the discretization the more precise is the percentile corresponding the largest Δ. However, the objective herein was to identify the general trend of Δ.

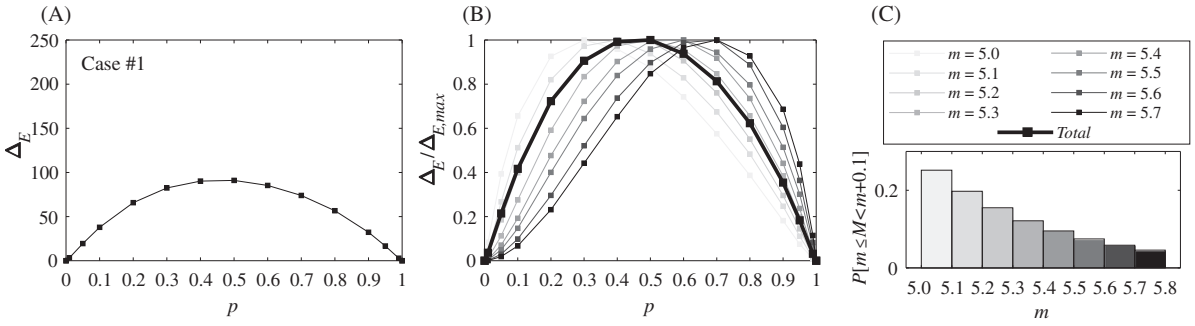

FIGURE 4 Effect of CH in MSPSHA in terms of Δ_E (A) and $\Delta_E/\Delta_{E,max}$ (B); magnitude distribution for the seismic source (C)

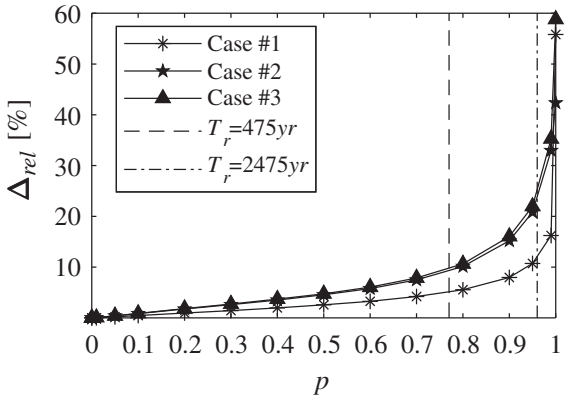

FIGURE 5 Comparison between the CH and the explicit approach in terms of nondimensional difference of variance

ordinate of such a curve (*Total* in the legend) is the sum of the ordinates of the normalized curves (i.e., each divided by the corresponding maximum) computed for bins of magnitude[†] (shades of gray in the figure), weighted by the probability of each magnitude bin, represented by the histogram in Figure 4C, that is, $P[m \le M < m + 0.1]$.

The shape of the *Total* curve in Figure 4B is due to the following two issues. First, the abscissa (i.e., the spectral acceleration thresholds at the sites) corresponding to the largest approximations due to CH increases with the considered magnitude. Second, since in the applications the magnitude distribution follows the GR model and thus $P[m \le M < m + 0.1]$ decreases with the increasing magnitude, the *Total* Δ_E is more affected by the lowest magnitude.

5.4 | Effect of CH in terms of nondimensional variance underestimation

What discussed so far is helpful in understanding the CH effects on the probabilistic distribution of the joint exceedances at the sites in a time interval. On the other hand, the comparison among the numerical values of Δ found in the considered cases cannot be used to draw general conclusions because the same value of the difference between $VAR[N(t, t + \Delta t)]$ and $VAR[N(t, t + \Delta t)]_{CH}$ may assume different relevance observing that $VAR[N(t, t + \Delta t)]$ (and $VAR[N(t, t + \Delta t)]_{CH}$ as well) strongly varies case by case. Thus, a nondimensional measure of the approximations is discussed in this section. Figure 5 provides, for each of the three cases, the values of the ratio defined as $\Delta_{rel} = \Delta/VAR[N(t, t + \Delta t)]$. It should be noted that such a ratio is independent on the Δt; see Equation (17). As shown, Δ_{rel} increases with the increasing thresholds and is comparable among the three different analyzed portfolio configurations (although the order of the approximations of the three cases shown in the previous sections is maintained). More specifically, when the thresholds are computed for $p = 0.78$, Δ_{rel} is equal to about 5% in case #1, and it is about 10% in both case #2 and case #3; for $p = 0.96$, Δ_{rel} increases to 12% in case #1 and it is about 24% for case #2 and case #3. The chosen values of p correspond, in the considered applications, to a return period (of the spectral acceleration thresholds) equal to $475yr$ ($p = 0.78$) and $2475yr$ ($p = 0.96$), the

[†] The curves are marginalized with respect to all possible earthquake locations.

same at all the sites (being $\nu = 0.0092$ events per year at each site; see Section 5.1). Thus, these results reveal that although the difference in terms of Δ appear to be numerically relevant (see Section 5.2), the relative variance underestimation due to CH is limited to 24% for return periods generally of interest to earthquake engineering, at least in the considered case-studies.

6 | EFFECT OF CH ON MULTI-SITE RISK ANALYSIS

Multi-site hazard is necessary for the seismic risk assessment of spatially distributed systems. It follows that the way in which the covariance matrix of the intensity measures at the sites is modelled may also affect risk. To give insights on this issue, $z \cdot s$ buildings (i.e., z structures located at each of the s sites) within a hypothetical portfolio are considered. Then, from the seismic risk assessment perspective, the analyst may be interested in characterizing the RV counting the number of failures due to the occurrence of one generic earthquake, N_f; i.e., to compute the probability that N_f is equal to an arbitrary number, say $n = 0, 1, \dots, z \cdot s$. This probability can be derived via the total probability theorem, as per Equation (18):

$$P\left[N_f = n\right] = \int_{Sa_1^1} \dots \int_{Sa_z^s} \int\int\int P\left[N_f = n \left| sa_1^1, \dots, sa_z^s, m, x, y \right.\right] \cdot f_{Sa_1^1,\dots,Sa_z^s|M,X,Y}\left(sa_1^1, \dots, sa_z^s \,|m, x, y\right) \times \\ \times f_{M,X,Y}(m, x, y) \cdot d\left(sa_1^1\right) \cdot \dots \cdot d\left(sa_z^s\right) \cdot dm \cdot dx \cdot dy \quad , \tag{18}$$

where $P[N_f = n|sa_1^1, \dots, sa_z^s, m, x, y]$ is the probability that n failures are observed conditional to $\{m, x, y\}$ and some values of ground motion spectral accelerations at the sites, while the $f_{Sa_1^1,\dots,Sa_z^s|M,X,Y}$ joint PDF is that introduced in Section 2.

Structural failure is often considered independent on $\{m, x, y\}$, if the ground motion intensity measure at the site is known. Accepting such an assumption, $P[N_f = n|sa_1^1, \dots, sa_z^s, m, x, y]$ can be re-written as $P[N_f = n|sa_1^1, \dots, sa_z^s]$. Moreover, under the hypothesis that, given the ground motion values at the sites, $sa_1^1, \dots, sa_z^s$, the structural failures are stochastically independent, $P[N_f = n|sa_1^1, \dots, sa_z^s]$ can be obtained as follows:

$$P\left[N_f = n \left| sa_1^1, \dots, sa_z^s \right.\right] = \int_{C_1^1} \dots \int_{C_z^s} I\left[\sum_{i=1}^{z}\sum_{j=1}^{s} I_{sa_i^j > c_i^j} = n\right] \cdot f_{C_1^1}\left(c_1^1\right) \cdot \dots \cdot f_{C_z^s}\left(c_z^s\right) \cdot d\left(c_1^1\right) \cdot \dots \cdot d\left(c_z^s\right). \tag{19}$$

In the equation, c_i^j is one realization of the structural capacity (C_i^j), in terms of spectral acceleration, for the $i-$th structure, $i = 1, \dots, z$, at the $j-$th site, $j = 1, \dots, s$; C_i^j is a RV and $f_{C_i^j}$ is the corresponding PDF. $I_{sa_i^j > c_i^j}$ is an indicator function that equals one if sa_i^j is larger than c_i^j and zero otherwise, while $I[\sum_{i=1}^{z}\sum_{j=1}^{s} I_{sa_i^j > c_i^j} = n]$ equals one if the sum of the indicator functions is equal to n and zero otherwise.

In the following, the implications of CH on risk results, in terms of number of failures jointly observed at the sites in fifty years, $N_f(t, t + 50)$, are investigated with reference to a simple application, in which the one-hundred sites and the input models introduced in Section 5 are considered. It is assumed that, at each site within the portfolio, two hypothetical structures are located; that is, $z = 2$. The spectral ordinates adopted to characterize the structural capacity are consistent with the spectral ordinates considered in case #3 of the previous section; see Figure 1 (this is to discuss risk approximations in the most severe case, in terms of hazard, among those considered above). For the purposes of this application, it is assumed that structural capacity of the $i-$th structure located at site j is modelled by means of a (often assumed) lognormal fragility function. Thus the $f_{Ca_i^j}$ PDF in Equation (19) is completely defined by the median (of the intensity measure causing failure), η_i^j, and the standard deviation (of the logarithm of the intensity causing failure), β_i^j, of the structural fragility. More specifically, for the $i-$th structure, $i = 1, 2$, located at site $j-$th site, $j = 1, \dots, 100$, η_i^j is arbitrarily assumed to be equal to the ground motion intensity measure threshold considered in the hazard analysis, sa_i^{j*}, (identified by the value of p, see Section 5.1). A value of β_i^j is arbitrarily assumed for each intensity measure considered for the structures: 0.4, 0.33, 0.25, 0.3, 0.28, 0.35 for PGA, Sa(0.6s), Sa(0.7s), Sa(0.8s), Sa(0.9s) and Sa(1s), respectively.

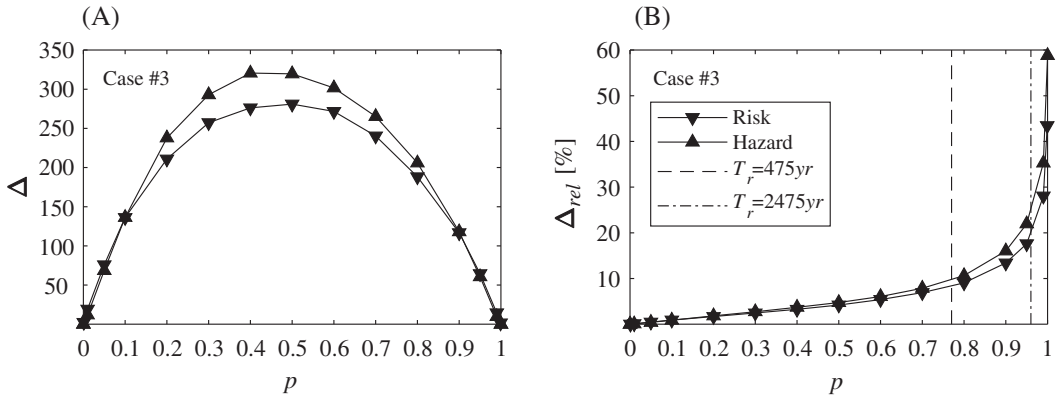

FIGURE 6 Differences between CH and explicit approach for hazard and risk analysis in terms of Δ (A) and Δ_{rel} (B)

Similar to Section 5, the effect of CH on risk results is quantified by comparing $VAR[N_f(t, t+50)]$ to $VAR[N_f(t, t+50)]_{CH}$. In both the MSPSHA approaches, the variance of the number of failures in the time interval is derived via Equation (1), in which N is replaced by N_f, and $P[N_f = n]$ is provided by Equation (18). Numerical simulations have been performed to approximate $P[N_f = n|sa_1^1, \dots, sa_z^s]$. In each simulation, c_i^j, for $i = 1, 2$ and $j = 1, \dots, 100$, which is randomly sampled from the lognormal fragility function with median η_i^j and standard deviation β_i^j, is compared with sa_i^j, that is, the element, for the $i-$th spectral ordinate at the $j-$th site, of the realization of $f_{Sa_1^1,\dots,Sa_z^s|M,X,Y}$, simulated according to explicit or CH-based MSPSHA (see Section 4). Thus, $P[N_f = n|sa_1^1, \dots, sa_z^s]$ is given by the number of simulations where the ground motion intensity is larger than structural fragility in n out of $z \cdot s$ cases, divided by the total number of simulations.

Figure 6A shows the effects of CH on risk analysis, in terms of $\Delta = VAR[N_f(t, t+50)] - VAR[N_f(t, t+50)]_{CH}$, considering the same p values of Section 5. In other words, the trend of Δ is explored varying the median of the fragility functions, while the standard deviation is maintained constant. In the figure, the analogous curve from case #3 (i.e., the curve shown in Figure 3C for $\Delta t = 50yr$) is also represented for comparison. It can be observed that, when CH-based MSPSHA is used, the variance of the number of failures is underestimated with respect to the explicit approach, similar to what observed for hazard analysis (i.e., neglecting the fragility functions). However, such an underestimation is comparatively less relevant in the case of risk. When the medians of the fragilities correspond to the ground motion intensity thresholds for p between 0.1 and 0.9, Δ can be up to about 30% lower than that found in the case of hazard analysis. Outside this range, the curves in the figure intersect, yet the values of Δ found in the case of risk and hazard assessment are comparable. In other words, considering that the acceleration causing structural failure is a RV tends to reduce the effects of the approximation of the covariance matrix of ground motion intensity measures, arisen when the CH approach is used for MSPSHA. At the very-low (-high) percentiles, risk and hazard appear to be both characterized by a low sensitivity to the MSPSHA procedure, when the CH implications are evaluated in terms of Δ. This is because, similar to what discussed in Section 5.2, when the median of the fragility function is very-low (-high), failures are observed at none of the (all) sites independently on the adopted MSPSHA procedure; therefore $VAR[N_f(t, t+\Delta t)]$ tends to be equal to $VAR[N_f(t, t+\Delta t)]_{CH}$ (and Δ tends to zero).

Finally, Figure 6B shows the nondimensional underestimation of failures variance, $\Delta_{rel} = \Delta / VAR[N_f(t, t+\Delta t)]$, together with the counterpart pertaining to hazard (i.e., the curve in Figure 5 for case #3). More specifically, referring to the same return periods considered in the previous section, it is found that, in the case of risk, Δ_{rel} reduces to 8% when the medians of fragilities correspond to the ground motion intensity thresholds with $T_r = 475yr$ according to classical PSHA, and to 18% for $T_r = 2475yr$.

7 | CONCLUSIONS

When an earthquake occurs in a region, the ground motion intensities at the sites in the hit area are not independent each other. This issue must be accounted for in multi-site PSHA, which requires to define the joint distribution of the intensity measures of interest at the sites, conditional to magnitude and earthquake location. The latter, in turn, requires

modeling the covariance matrix of the intensity measures at the sites in one earthquake, which consists of spatial-, cross-, and spatial cross-correlations.

In this study, two different strategies for MSPSHA were considered, assuming spectral accelerations as the intensity measures. One approach, herein denoted as explicit, models all possible correlations among residuals of the GMPE at the sites. The other one relies on the concept of conditional hazard, originally developed for single-site vector-valued PSHA. It allows to derive the joint PDF of multiple spectral accelerations at the sites in one earthquake needed for MSPSHA, yet defining only part of the whole covariance matrix of the spectral accelerations, while the rest is approximated in accordance with the hypotheses of the approach. More specifically, the CH-based approach does not need a spatial cross-correlation model being available.

The objective of this paper was to recall the CH-based MSPSHA, first. Then, its implications on the definition of the covariance matrix of spectral accelerations at the sites in one earthquake were analytically discussed. Finally, the effects of CH on some MSPSHA results, and ultimately on multi-site risk analysis, were quantitatively investigated, with reference to three case-studies chosen to provide conclusions as general as possible. Results of CH and explicit MSPSHA were compared in terms of number of exceedances of selected ground motion intensity thresholds jointly observed at the sites in different time intervals. All the three case-studies referred to one-hundred sites in the district of Naples (southern Italy) and in each of them $Sa(1s)$ was considered as primary intensity measure, at all sites, because it is the largest period spectral acceleration, as suggested by literature for CH-based MSPSHA. In case #1, PGA, which is the less correlated with $Sa(1s)$, was the ground motion intensity measure of interest assumed for 25% of sites, whereas, for the other sites, spectral accelerations to vibration periods between 0.6 and 1s were considered. In case #2, PGA was assigned at 61% of the sites. Case #3 extends case #1 by considering two thresholds per site: the first threshold is the same considered in case #1, the second is PGA for all the sites. To avoid the dependence of the presented results on the rate of earthquakes on the source, the thresholds for all the sites were selected to be representative of the same non-exceedance probability (computed via single-site PSHA) given the occurrence of one generic earthquake on the source, p. In the following, some final remarks, which are specific for the considered case-study, are given.

- CH approach implies an underestimation of the variance of number of threshold exceedances at the sites. The difference between the variances obtained through the two approaches increases linearly with the width of the time interval in which exceedances are counted. On the other hand, given the width, such an underestimation shows a non-monotonic trend with p. The difference of the variances increases for the increasing thresholds, reaches a maximum (whose value depends on the case, to follow) when p is about 0.5, and decreases for larger values of$p$. If p tends to zero or one, the variance differences tend to zero, for explained reasons.
- Given the width of the time interval, the variance underestimation varies with the intensity measures considered at each site. For example, for Δt equal to 150 years, case #1 shows a maximum value of Δ equal to about 100. Increasing the number of sites referring to PGA, i.e., case #2, Δ increases to about 200; in the case of two thresholds per site (case #3), Δ can even approach to one thousand, depending on the thresholds. The seemingly large values of Δ resulting from the applications are so because of the large number of considered sites that determines a large number of expected exceedances in the considered time intervals.
- The effects of CH were also investigated in relative terms, that is, by quantifying $\Delta/VAR[N(t, t+\Delta t)]$. Such a ratio is independent of Δt, it increases with the thresholds at the sites, but it generally assumes limited values. In case #1, it is about 5% when the thresholds have, individually, $p = 0.78$ and 12% for $p = 0.96$. In both case #2 and case #3, it is equal to about 10% and 24% for $p = 0.78$ and $p = 0.96$, respectively. According to the considered source model, the thresholds corresponding to $p = 0.78$ have $T_r = 475yr$ at each site, whereas $T_r = 2475yr$ corresponds to $p = 0.96$.
- When multi-site risk analysis is considered, variance underestimation due to CH is reduced with respect to the result of the corresponding multi-site hazard analysis alone. Assuming the fundamental periods of the structures consistent with the spectral ordinates considered in case #3, if the medians of fragilities are equal to the ground motion intensity thresholds with $T_r = 475yr$, the relative underestimation decreases from 10% (hazard) to 8% (risk), and from 24% to 18% for $T_r = 2475yr$.

ACKNOWLEDGEMENTS

The work presented in this article was developed within the H2020-SC5-2019 Real-time Earthquake Risk Reduction for a Resilient Europe (RISE) project, Grant Agreement 821115. The help of Massimiliano Giorgio (Università degli Studi di Napoli Federico II), in deriving the implicit correlations of the conditional hazard approach, is also acknowledged.

DATA AVAILABILITY STATEMENT

Data sharing not applicable to this article as no datasets were generated or analyzed during the current study.

ORCID

Pasquale Cito https://orcid.org/0000-0001-6603-8106
Eugenio Chioccarelli https://orcid.org/0000-0002-8990-3120
Iunio Iervolino https://orcid.org/0000-0002-4076-2718

REFERENCES

1. Cornell CA. Engineering seismic risk analysis. *Bull Seismol Soc Am*. 1968;58(5):1583-1606.
2. Mc Guire RK. Seismic Hazard And Risk Analysis. *Earthq Eng Res Institute, Oakland, CA*. 2004.
3. Esposito S, Iervolino I. Spatial Correlation of Spectral Acceleration in European Data. *Bull Seismol Soc Am*. 2012;102(6):2781-2788. https://doi.org/10.1785/0120120068
4. Esposito S, Iervolino I, d'Onofrio A, Santo A, Cavalieri F, Franchin P. Simulation-Based Seismic Risk Assessment of Gas Distribution Networks. *Comput Civ Infrastruct Eng*. 2015;30(7):508-523. https://doi.org/10.1111/mice.12105
5. Esposito S, Botta A, De Falco M, et al. Seismic risk analysis of a data communication network. *Sustain Resilient Infrastruct*. 2022. https://doi.org/10.1080/23789689.2021.2004646. press.
6. Mc Guire RK. Seismic risk to lifeline systems: critical variables and sensitivities. *Proc 9th World Conf Earthq Eng Tokyo, Japan*. 1988.
7. Eguchi RT. Seismic hazard input for lifeline systems. *Struct Saf*. 1991;10:193-198.
8. Weatherill GA, Silva V, Crowley H, Bazzurro P. Exploring the impact of spatial correlations and uncertainties for portfolio analysis in probabilistic seismic loss estimation. *Bull Earthq Eng*. 2015;13:957-981. https://doi.org/10.1007/s10518-015-9730-5
9. Markhvida M, Ceferino L, Baker JW. Modeling spatially correlated spectral accelerations at multiple periods using principal component analysis and geostatistics. *Earthq Eng Struct Dyn*. 2018;47(5):1107-1123. https://doi.org/10.1002/eqe.3007
10. Inoue T, Cornell CA. Seismic hazard analysis of multi-degree-of-freedom structures. *Reliab Mar Struct*. 1990. RMS-8-Sta. purl.stanford.edu/hw982bg3509.
11. Baker JW, Jayaram N. Correlation of Spectral Acceleration Values from NGA Ground Motion Models. *Earthq Spectra*. 2008;24:299-317. https://doi.org/10.1193/1.2857544
12. Jayaram N, Baker JW. Correlation model for spatially distributed ground-motion intensities. *Earthq Eng Struct Dyn*. 2009;38(15):1687-1708. https://doi.org/10.1002/eqe.922
13. Bradley BA, Lee DS. Accuracy of approximate methods of uncertainty propagation in seismic loss estimation. *Struct Saf*. 2010. https://doi.org/10.1016/j.strusafe.2009.04.001
14. Bradley BA. Empirical Correlations between Peak Ground Velocity and Spectrum-Based Intensity Measures. *Earthq Spectra*. 2012;28:17-35. https://doi.org/10.1193/1.3675582
15. Goda K, Hong HP. Spatial Correlation of Peak Ground Motions and Response Spectra. *Bull Seismol Soc Am*. 2008;98(1):354-365. https://doi.org/10.1785/0120070078
16. Loth C, Baker JW. A spatial cross-correlation model of spectral accelerations at multiple periods. *Earthq Eng Struct Dyn*. 2013;42(3):397-417. https://doi.org/10.1002/eqe.2212
17. Iervolino I, Giorgio M, Galasso C, Manfredi G. Conditional Hazard Maps for Secondary Intensity Measures. *Bull Seismol Soc Am*. 2010;100(6):3312-3319. https://doi.org/10.1785/0120090383
18. Bazzurro P, Cornell CA. Vector-valued probabilistic seismic hazard analysis (VPSHA). *Proc 7th US Natl Conf Earthq Eng Boston, USA*. 2002.
19. Cito P, Chioccarelli E, Iervolino I. Comparing alternative models for multisite probabilistic seismic risk analysis. *Proc 13th Int Conf Appl Stat Probab Civ Eng ICASP13 Seoul, South Korea*. 2019.
20. Iervolino I, Giorgio M, Cito P. The effect of spatial dependence on hazard validation. *Geophys J Int*. 2017;209(3):1363-1368. https://doi.org/10.1093/gji/ggx090
21. Giorgio M, Iervolino I. On Multisite Probabilistic Seismic Hazard Analysis. *Bull Seismol Soc Am*. 2016;106(3):1223-1234. https://doi.org/10.1785/0120150369
22. Kotha SR, Weatherill G, Bindi D, Cotton F. A regionally-adaptable ground-motion model for shallow crustal earthquakes in Europe. *Bull Earthq Eng*. 2020;18(9):4091-4125. https://doi.org/10.1007/s10518-020-00869-1
23. Kuehn NM, Abrahamson NA. Spatial correlations of ground motion for non-ergodic seismic hazard analysis. *Earthq Eng Struct Dyn*. 2020;49(1):4-23. https://doi.org/10.1002/eqe.3221
24. Lavrentiadis G, Abrahamson NA, Nicolas KM, et al. Overview and introduction to development of non-ergodic earthquake ground-motion models. *Bull Earthq Eng*. 2022. https://doi.org/10.1007/s10518-022-01485-x
25. Kramer SL. *Geotechnical earthquake engineering*. Prentice-Hall, Inc; 1996.
26. Kotha SR, Bindi D, Cotton F. Site-corrected magnitude- and region- dependent correlations of horizontal peak spectral amplitudes. *Earthq Spectra*. 2017;33(4):1415-1432. https://doi.org/10.1193/091416EQS150M
27. Park J, Bazzurro P, Baker JW. Modeling spatial correlation of ground motion Intensity Measures for regional seismic hazard and portfolio loss estimation. *Proc 10th Int Conf Appl Stat Probab Civ Eng (ICASP10), Tokyo, Japan*. 2007.

28. Malhotra PK. Seismic Design Loads from Site-Specific and Aggregate Hazard Analyses. *Bull Seismol Soc Am*. 2008;98(4):1849-1862. https://doi.org/10.1785/gssrl.78.4.415
29. Meletti C, Galadini F, Valensise G, et al. A seismic source zone model for the seismic hazard assessment of the Italian territory. *Tectonophysics*. 2008;450:85-108. https://doi.org/10.1016/j.tecto.2008.01.003
30. Barani S, Spallarossa D, Bazzurro P. Disaggregation of Probabilistic Ground-Motion Hazard in Italy. *Bull Seismol Soc Am*. 2009;99(5):2638-2661. https://doi.org/10.1785/0120080348
31. Gutenberg B, Richter CF. Frequency of earthquakes in California. *Bull Seismol Soc Am*. 1944;34(4):185-188. https://doi.org/10.1785/BSSA0340040185
32. Akkar S, Bommer JJ. Empirical Equations for the Prediction of PGA, PGV, and Spectral Accelerations in Europe, the Mediterranean Region, and the Middle East. *Seismol Res Lett*. 2010;81(2):195-206. https://doi.org/10.1785/gssrl.81.2.195
33. Joyner WB, Boore DM. Peak horizontal acceleration and velocity from strong-motion records including records from the 1979 Imperial Valley, California, earthquake. *Bull Seismol Soc Am*. 1981;71(6):2011-2038. https://doi.org/10.1785/BSSA0710062011
34. Montaldo V, Faccioli E, Zonno G, Akinci A, Malagnini L. Treatment of ground-motion predictive relationships for the reference seismic hazard map of Italy. *J Seismol*. 2005;9:295-316. https://doi.org/10.1007/s10950-005-5966-x
35. Chioccarelli E, Cito P, Iervolino I, Giorgio M. REASSESS V2.0: software for single- and multi-site probabilistic seismic hazard analysis. *Bull Earthq Eng*. 2018. https://doi.org/10.1007/s10518-018-00531-x
36. Weiss NA. A Course in Probability. *Addison–Wesley*. 2005:385-386.

How to cite this article: Cito P, Chioccarelli E, Iervolino I. Conditional hazard for simplified multi-site seismic hazard and risk analyses. *Earthquake Engng Struct Dyn*. 2023;52:482–499. https://doi.org/10.1002/eqe.3769